

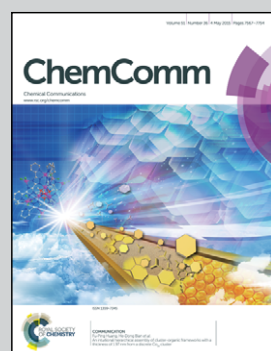
Showcasing research from the "Inorganic Membrane Research Laboratory", Advanced Membranes and Porous Materials Center, Division of Physical Science and Engineering, King Abdullah University of Science and Technology, Kingdom of Saudi Arabia

A rationally designed amino-borane complex in a metal organic framework: a novel reusable hydrogen storage and size-selective reduction material

Amino-borane covalently bonded into a stable UiO-66 metal organic framework can be used as a reversible hydrogen storage material and a size-selective reduction agent.

Nano-confinement upgrades material properties. In their communication on pp. 7610–7613, Xinbo Wang, Linhua Xie, Kuo-Wei Huang and Zhiping Lai reveal that the uniform porous structure of a metal organic framework can improve hydrogen release performance and offers size selectivity to the chemically bonded amino borane groups inside the framework.

### As featured in:



See Zhiping Lai et al.,  
*Chem. Commun.*, 2015, **51**, 7610.



Cite this: *Chem. Commun.*, 2015, 51, 7610

Received 11th January 2015,  
Accepted 23rd February 2015

DOI: 10.1039/c5cc00193e

[www.rsc.org/chemcomm](http://www.rsc.org/chemcomm)

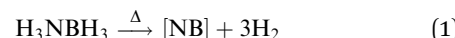
## A rationally designed amino-borane complex in a metal organic framework: a novel reusable hydrogen storage and size-selective reduction material<sup>†</sup>

Xinbo Wang, Linhua Xie, Kuo-Wei Huang and Zhiping Lai\*

**A novel amino-borane complex inside a stable metal organic framework was synthesized for the first time. It releases hydrogen at a temperature of 78 °C with no volatile contaminants and can be well reused. Its application as a size-selective reduction material in organic synthesis was also demonstrated.**

Over the past several decades, hydrogen has emerged as an ideal successor to gasoline because of its lightweight and clean combustion properties.<sup>1</sup> The current hydrogen storage approaches such as high pressure and cryogenics, however, have suffered disadvantages including large bulky size as well as high safety risks. One of the milestones for hydrogen storage was the development of light-weight solids that could reversibly release H<sub>2</sub>. Especially ammonia-borane (AB) (NH<sub>3</sub>BH<sub>3</sub>), which releases hydrogen upon heating according to reaction (1), is considered to be a promising hydrogen storage material due to its stability and high gravimetric content of hydrogen (19.6 wt%).<sup>2</sup> However, several issues still need to be addressed before it can be used, involving decreasing the dehydrogenation temperature below 85 °C, and preventing the formation of volatile by-products, such as borazine (N<sub>1</sub>B<sub>x</sub>H<sub>x</sub>), ammonia, and diborane. The current methods to overcome these issues can be summarized into three general approaches. One is to chemically modify AB in the form of RNHBH<sub>3</sub>,<sup>3–6</sup> where R can be an alkyl group, heterocycles, ionic liquid, or a metal cation. A second approach is the catalytic dehydrogenation of AB with different mechanistic pathways,<sup>7–11</sup> including activation by base, acid, ionic liquids, transition metal complexes, or metal nanoparticles. A third approach is to physically load AB into microporous materials such as mesoporous silicas<sup>12</sup> and metal organic frameworks (MOFs).<sup>13–21</sup> The nano-confinement as well as the unique interactions between AB and the framework were found

to be beneficial to reduce the dehydrogenation temperature and the formation of by-products.



Since AB can be formed by the reaction between borane and ammonia, so if a microporous material is functionalized with amino groups, then borane should be able to react with the amino group to form the amino-borane complex inside the framework. Based on this idea, here we report for the first time the storage of borane in a stable amino-substituted MOF, UiO-66-NH<sub>2</sub>, and its reversible release of hydrogen. Our approach can be explained as follows. Borane first adsorbs on UiO-66-NH<sub>2</sub> by reacting with the amino group to form an amino-borane complex inside the UiO-66 structure, which is named as UiOAB. Hydrogen is then released from UiOAB by thermolysis. The dehydrogenation product is removed by methanol and UiO-66-NH<sub>2</sub> is regenerated. The strong covalent bonding between borane and amino groups as well as the nano confinement will improve the borane loading rate, reduce the dehydrogenation temperature and form volatile species during the process of dehydrogenation. Furthermore, the isolated and uniformly distributed amino binding sites will enhance the hydrogen release kinetics and prevent polymerization of dehydrogenation products, so they can be easily reacted and then dissolved in methanol and be removed. As a result, the dehydrogenation temperature was found to be as low as 78 °C and no volatile by-product was generated during this process.

The recently developed MOFs are very attractive for adsorption not only because of their high surface area, high porosity, and tunable pore size, but also because of their easy functionality that allows to introduce functional groups to their frameworks by design.<sup>22,23</sup> In fact, functional groups have been widely used to enhance the adsorption loading rate, and to fine-tune the adsorption/desorption kinetics. A number of amino substituted MOFs have been reported in the literature,<sup>24–26</sup> such as IRMOF-3, DMOF-1-NH<sub>2</sub>, UCMC-1-NH<sub>2</sub> and UiO-66-NH<sub>2</sub>. Therefore, our approach in principle can serve as a general method to utilize MOFs as a platform to store borane. However, UiO-66-NH<sub>2</sub> is of

Division of Physical Science and Engineering, King Abdullah University of Science and Technology (KAUST), Thuwal, 23955-6900, Saudi Arabia.

E-mail: [zhiping.lai@kaust.edu.sa](mailto:zhiping.lai@kaust.edu.sa)

† Electronic supplementary information (ESI) available: Experimental details and additional figures. See DOI: [10.1039/c5cc00193e](https://doi.org/10.1039/c5cc00193e)



particular interest because of its good stability.  $\text{UiO-66-NH}_2$  is constructed with hexameric  $\text{Zr}_6\text{O}_4(\text{OH})_4(-\text{CO}_2)_{12}$  clusters and 2-amino-terephthalic acid containing tetrahedral (approximately 8 Å) and octahedral cavities (approximately 11 Å) accessible by microporous triangular windows (approximately 6 Å).<sup>27</sup> The framework of  $\text{UiO-66-NH}_2$  is stable at temperatures up to 300 °C. It is also stable in most organic solvents, water, and acidic aqueous solutions due to strong bonding between oxophilic  $\text{Zr}^{4+}$  ions and carboxylate groups of the ligands as well as the inherent high connectivity of its framework.<sup>26</sup> The good stability of  $\text{UiO-66-NH}_2$  has enabled its wide range of applications in such as post-synthetic modifications,<sup>26</sup> metal nanoparticle dispersions,<sup>28</sup> and direct usage in heterogeneous catalysis.<sup>29</sup>

The  $\text{UiOAB}$  complex can also find potential usage in organic synthesis. Borane–amine adducts are important stock compounds that have found broad range of applications in academic and industrial processes, such as hydroboration of olefins, reduction of carbonyl compounds, and as precursors for polyaminoboranes.<sup>30</sup> Unlike other diborane compounds, such as borane–tetrahydrofuran ( $\text{BH}_3\text{-THF}$ ) and borane–dimethyl sulfide ( $\text{BH}_3\text{-Me}_2\text{S}$ ), that often suffer low stability, high volatility, flammability and sometimes an unpleasant odor, borane–amine adducts are typically stable in air, easy to handle, and environmentally benign<sup>31</sup> due to a tighter boron–nitrogen bond. Although enantioselective reduction of carbonyl compounds has been well established with borane reagents such as the CBS-reduction reaction,<sup>32</sup> to the best of our knowledge, a general substrate-size-selective protocol has not been previously reported for either borane or borane–amine adducts. The  $\text{UiOAB}$  complex containing borane–amine substructures inside its uniform cavity may offer a good opportunity to achieve this goal with a molecular sieving effect that has been observed in other MOFs and zeolite systems.<sup>33–35</sup> To demonstrate this idea, the selective reduction of aldehyde compounds with different molecular sizes was selected as a prototype system.

The MOF-amino-borane complex, namely  $\text{UiOAB}$ , was obtained by simply treating  $\text{UiO-66-NH}_2$  with borane in diethyl ether medium (see the Experimental details in the ESI†). Elemental analysis using ICP-OES (Table S1, ESI†) revealed that 4.55% of borane was loaded in  $\text{UiOAB}$ , which is equivalent to 1.2 borane per amine group inside the framework. The more than stoichiometric amount of borane loading indicates that there are at least two types of amine-borane complexes formed. The solid state  $^{11}\text{B}$  NMR of  $\text{UiOAB}$  (Fig. 1, right) contains two main peaks at  $-17.2$  and  $-22.5$  ppm, which indicated that there were two types of boron states corresponding to  $-\text{NH}_2\text{BH}_3$

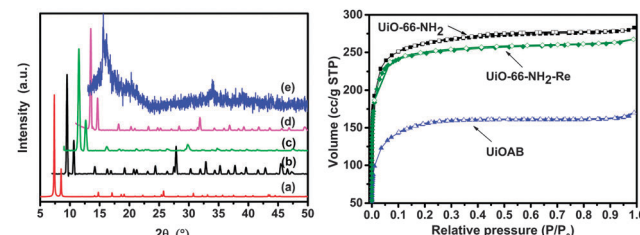


Fig. 2 Left: PXRD patterns of  $\text{UiO-66-NH}_2$  at different stages. Each pattern was shifted 2 degrees from each other to the right for clarity. (a) Simulated  $\text{UiO-66-NH}_2$  pattern from cif-file CCDC 837796, (b) as-synthesized  $\text{UiO-66-NH}_2$ , (c) as-synthesized  $\text{UiOAB}$ , (d)  $\text{UiO-66-NH}_2\text{-Re}$ , and (e)  $\text{UiOAB}$  after TGA-QMS analysis during which  $\text{UiOAB}$  was heated from room temperature to 200 °C at a ramping rate of 1 °C min<sup>-1</sup> under 20 ml min<sup>-1</sup> argon flow. Right:  $\text{N}_2$  uptake isotherm at 77 K; adsorption (filled) and desorption (open).

and  $-\text{NH}_2\text{B}_2\text{H}_5$ , respectively. The FTIR spectrum (Fig. 1, left) of  $\text{UiOAB}$  exhibited a new broad peak near 2300 cm<sup>-1</sup>, which is due to the characteristic peak of B–H symmetric stretching vibrations and indicates that  $\text{UiO-66-NH}_2$  has reacted with borane to yield  $\text{UiOAB}$ . After thermolysis and washing with methanol, this band disappeared in  $\text{UiO-66-NH}_2\text{-Re}$ . In fact, the FTIR spectrum of  $\text{UiO-66-NH}_2\text{-Re}$  contained nearly the same peaks as  $\text{UiO-66-NH}_2$ . In addition, the ICP-OES and  $^{11}\text{B}$  NMR spectrum of  $\text{UiO-66-NH}_2\text{-Re}$  exhibit no additional signals for boron, indicating that the adsorbed borane was completely removed. All of these characterization results confirmed that the desired MOF-amino-borane complex  $\text{UiOAB}$  was formed.

Borane is a well-known reductant that may react with carboxylate groups, which is one of the main building blocks of  $\text{UiO-66-NH}_2$ , and possibly leads to a structural collapse.<sup>36</sup> Therefore, PXRD was recorded in each step to monitor the structural change. The PXRD pattern (Fig. 2, left) of  $\text{UiO-66-NH}_2$  matches well with simulated  $\text{UiO-66}$ . The XRD patterns of  $\text{UiOAB}$  and  $\text{UiO-66-NH}_2\text{-Re}$  are nearly identical to that of  $\text{UiO-66-NH}_2$ . All of the patterns have sharp diffraction peaks and flat baselines, which indicate that the synthesized  $\text{UiO-66-NH}_2$  powder exhibited good crystallinity and remained intact during borane loading and hydrogen release. However, the PXRD peaks of  $\text{UiOAB}$  after TGA analysis during which it was heated to 200 °C and maintained at this temperature for 6 hours, nearly disappeared, which indicates that the structure collapsed at this temperature. This temperature is much lower than that reported in the literature<sup>26</sup> (*i.e.*, approximately 300 °C, which was determined from TGA analysis). The lower decomposition temperature is most likely due to two reasons. First, the structural collapse temperature determined by PXRD is typically lower than that determined by TGA analysis. Second, boron can promote radical oxidation of the carboxylate group in the framework, which has been commonly observed in organic chemistry.<sup>37,38</sup> Nevertheless, since the temperatures for borane loading and hydrogen release (which will be discussed in the next paragraph) are much below 200 °C,  $\text{UiOAB}$  is stable enough for borane storage and reuse.

Fig. 3 shows the SEM images of the crystal morphologies at different stages. The as-synthesized  $\text{UiO-66-NH}_2$  particles have an octahedral morphology with an average particle size of 1 micrometer.

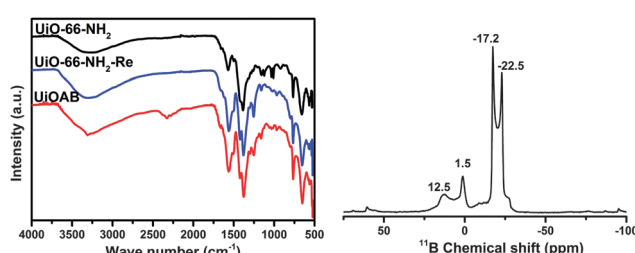


Fig. 1 Left: FTIR spectra of  $\text{UiO-66-NH}_2$  (black),  $\text{UiOAB}$  (red) and  $\text{UiOAB}$  after thermolysis at 90 °C and washing with methanol, which is referred to as  $\text{UiO-66-NH}_2\text{-Re}$  (blue). Right: solid state  $^{11}\text{B}$  NMR of  $\text{UiOAB}$ .



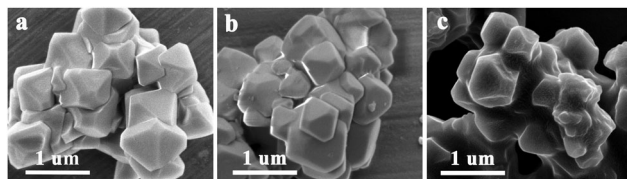


Fig. 3 SEM images of (a)  $\text{UiO-66-NH}_2$ , (b)  $\text{UiOAB}$ , and (c)  $\text{UiO-66-NH}_2\text{-Re}$ .

The size and morphology were well preserved in  $\text{UiOAB}$ . However, some particles were broken into approximately half their original size after hydrogen release in  $\text{UiO-66-NH}_2\text{-Re}$ , which is most likely due to the volume change that occurs during the adsorption–desorption process. This volume change is a common challenge for the adsorption process. The BET surface area and pore volume of the as-synthesized  $\text{UiO-66-NH}_2$  was determined to be  $976 \text{ m}^2 \text{ g}^{-1}$  and  $0.4377 \text{ cm}^3 \text{ g}^{-1}$ , respectively, which is similar to the values reported in the literature.<sup>26</sup> After loading with borane, these values sharply decreased to  $298 \text{ m}^2 \text{ g}^{-1}$  and  $0.1618 \text{ cm}^3 \text{ g}^{-1}$ , respectively, in  $\text{UiOAB}$ , which demonstrated that the pores were largely occupied by borane. For  $\text{UiO-66-NH}_2\text{-Re}$ , these two values recovered to  $834 \text{ m}^2 \text{ g}^{-1}$  and  $0.4136 \text{ cm}^3 \text{ g}^{-1}$ , respectively. Therefore, most of the pores were re-opened after hydrogen release. Both the BET adsorption (Fig. 2, right) and PXRD data demonstrated the excellent stability and reusability of  $\text{UiO-66-NH}_2$  in our hydrogen production strategy.

Thermogravimetric analysis coupled with quadrupole mass spectrometry (TGA-QMS) was used to investigate hydrogen release (Fig. 4) from both neat AB and  $\text{UiOAB}$ . The results indicated that neat AB releases hydrogen mainly at two temperatures. The first temperature is at  $114^\circ\text{C}$ , and the second at  $149^\circ\text{C}$ . Neat AB also produces a large quantity of volatile by-products, such as ammonia, diborane, and borazine. In contrast, the dehydrogenation of  $\text{UiOAB}$  started at a temperature below  $50^\circ\text{C}$ , which is the lowest detectable limit of the equipment, and only one temperature peak was observed at  $78^\circ\text{C}$ . Therefore, in comparison to neat AB, the dehydrogenation temperature was significantly reduced. In contrast to the approach where AB is physically absorbed inside the mesoporous silica or MOF channels, the amine-borane complex of  $\text{UiOAB}$  can be considered to be a single point of molecular AB. This may explain why there is only one hydrogen releasing peak in our system. The strong chemical bonding between borane and amino groups also explains why there are no volatile by-products generated during the decomposition process.

The area under the two hydrogen peaks of neat AB in Fig. 4 is equivalent to approximately 10 wt% of hydrogen, as reported in the literature.<sup>13</sup> Using this as a reference, the total amount of hydrogen released from  $\text{UiOAB}$  is approximately 2.2 wt%. Because the borane loading in  $\text{UiOAB}$  is 4.55%, as determined by ICP-OES, therefore, almost all hydrogen in borane adsorbed in  $\text{UiOAB}$  are released. Strong reducing agents such as  $\text{LiAlH}_4$  and hydrazine and harsh conditions are always required to regenerate AB from the dehydrogenation products of poly-borazylene.<sup>39</sup> While in our system, the AB complexes are spatially separated by each other so that polymerization is fundamentally avoided. After dehydrogenation,  $\text{UiO-66-NH}_2$  can be regenerated by simply soaking in methanol,

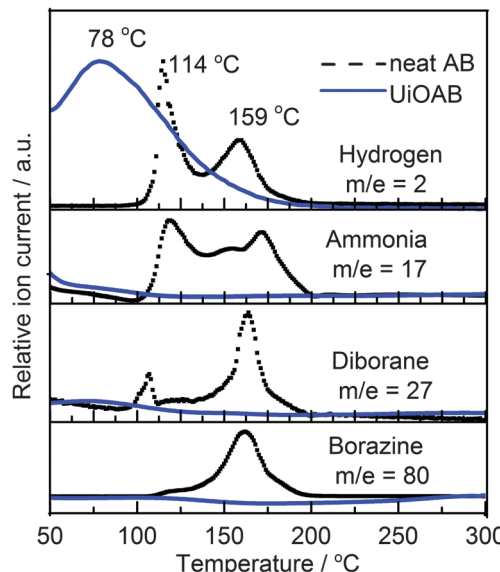


Fig. 4 TGA-QMS spectra of neat AB (black dashed line) and  $\text{UiOAB}$  (blue solid line) during the dehydrogenation process.

as confirmed by IR, solid  $^{11}\text{B}$  NMR/MAS,  $\text{N}_2$  isothermal physisorption as well as by SEM as above mentioned. Table S2 summarizes the reported hydrogen release results from AB physically loaded in different MOF systems. Compared to most reported results, our work showed a higher hydrogen loading rate and a lower hydrogen release temperature. From all these results it can be clearly seen that no matter whether AB is physically loaded, as reported in the literature, or chemically bonded, as reported in our studies, the nano-confinement provided by the MOF structure played an important role in reducing the hydrogen release temperature and the generation of contaminants.

DFT calculations of the  $\text{N}_2$  physisorption isotherm data indicated a decrease in pore size from  $7.3 \text{ \AA}$  in  $\text{UiO-66-NH}_3$  to  $5.3 \text{ \AA}$  in  $\text{UiOAB}$ . This pore size is bigger than the kinetic diameter of linear alkyl aldehydes such as propanal ( $\sim 4.7 \text{ \AA}$ ) and butyral ( $\sim 5.0 \text{ \AA}$ ), but smaller than aromatic aldehydes such as benzaldehyde ( $\sim 5.9 \text{ \AA}$ ) and phenanthrene-9-carbaldehyde ( $\sim 8.9 \text{ \AA}$ ). So a substrate size selective reduction was expected and demonstrated. The aldehyde reduction reactions were conducted in methanol at  $60^\circ\text{C}$  for 4 hours. Under these conditions our control experiments showed that when borane, sodium borane hydride and ammonia borane were used as reducing agents all these aldehydes were converted quantitatively to the related alcohol products without notable selectivity. However, when  $\text{UiOAB}$  was used as a reducing agent, the results in Table 1 show that for small sized propanal and butyral, the conversion is more than 95%, but for large benzaldehyde, the conversion decreased to 35%. The results indicate that propanal and butyral can freely enter the pores of  $\text{UiOAB}$ . Benzaldehyde can also enter the pores, presumably due to the structural flexibility that commonly observed in the MOF structure, but in much slow rate. For this reaction we further extended the reaction time to another 12 hours. Since as shown in Fig. 4,  $\text{UiOAB}$  starts to decompose at a temperature below  $60^\circ\text{C}$ , to maintain enough



Table 1 Substrate-specific reduction of aldehydes using UiOAB

Entry	Substrates	Product	Conversion <sup>a</sup> (%)	UiOAB
				MeOH, 60 °C, 4h
1			99	
2			95	
3			35 (80) <sup>b</sup>	
4			0	
5			90/2	

<sup>a</sup> Conversion determined by GC. <sup>b</sup> The reaction was continued after 4 hours by adding another 1 eq. of UiOAB and extending the reaction time for another 12 hours.

amount of UiOAB in the reaction medium, we added another 1 eq. of UiOAB. At the end, the conversion of benzaldehyde was increased to 80%. When a more steric bulky molecule, phenanthrene-9-carbaldehyde, is used, no product was detected. To further demonstrate the size-selective effect, a mixture of propanal and benzaldehyde in 1:1 mole ratio was studied under the standard reaction conditions (Table 1, entry 5). A high product selectivity of 49 was obtained. All of these results clearly demonstrated the potential usage of UiOAB as a size-selective reduction agent for organic synthesis.

In summary, a microporous metal-organic framework UiOAB, which contains amino-borane complexes chemically bonded to its internal framework, was rationally designed and synthesized. This novel material can act as both a reusable hydrogen chemical storage material and a size-selective reduction agent. The dehydrogenation temperature was substantially decreased from 114 °C to 78 °C compared to neat AB, and also no volatile by-products were generated during the process. The enhancement in dehydrogenation kinetics and inhibition of volatile compounds confirmed the nano-confinement effect of the spatial isolation by chemical immobilization. In the reduction reactions, large substrates exhibited significantly reduced activities and conversions compared to small substrates, demonstrating that the reaction occurs primarily within the pores, which leads to a sharp molecular sieving effect.

Financial support from KAUST Competitive Grant URF/1/1378 and Baseline fund BAS/1/1375 is gratefully acknowledged.

## References

1. L. Schlapbach and A. Zuttel, *Nature*, 2001, **414**, 353.
2. F. H. Stephens, V. Pons and R. T. Baker, *Dalton Trans.*, 2007, 2613.
3. M. E. Bowden, I. W. Brown, G. J. Gainsford and H. Wong, *Inorg. Chim. Acta*, 2008, **361**, 2147.
4. S. Li, Z. Tang, Q. Gong, X. Yu, P. R. Beaumont and C. M. Jensen, *J. Mater. Chem.*, 2012, **22**, 21017.
5. G. Chen, L. N. Zakharov, M. E. Bowden, A. J. Karkamkar, S. M. Whittemore, E. B. Garner, T. C. Mikulas, D. A. Dixon, T. Autrey and S.-Y. Liu, *J. Am. Chem. Soc.*, 2015, **1**, 134.
6. W. Luo, P. G. Campbell, L. N. Zakharov and S.-Y. Liu, *J. Am. Chem. Soc.*, 2011, **133**, 19326.
7. F. H. Stephens, R. T. Baker, M. H. Matus, D. J. Grant and D. A. Dixon, *Angew. Chem., Int. Ed.*, 2007, **46**, 746.
8. J. M. Yan, X. B. Zhang, S. Han, H. Shiota and Q. Xu, *Angew. Chem., Int. Ed.*, 2008, **47**, 2287.
9. M. E. Bluhm, M. G. Bradley, R. Butterick, U. Kusari and L. G. Sneddon, *J. Am. Chem. Soc.*, 2006, **128**, 7748.
10. D. W. Himmelberger, C. W. Yoon, M. E. Bluhm, P. J. Carroll and L. G. Sneddon, *J. Am. Chem. Soc.*, 2009, **131**, 14101.
11. R. J. Keaton, J. M. Blacquiere and R. T. Baker, *J. Am. Chem. Soc.*, 2007, **129**, 1844.
12. A. Gutowska, L. Y. Li, Y. S. Shin, C. M. M. Wang, X. H. S. Li, J. C. Linehan, R. S. Smith, B. D. Kay, B. Schmid, W. Shaw, M. Gutowski and T. Autrey, *Angew. Chem., Int. Ed.*, 2005, **44**, 3578.
13. L. Gao, C.-Y. V. Li, H. Yung and K.-Y. Chan, *Chem. Commun.*, 2013, **49**, 10629.
14. S. Gadielli, J. Ford, W. Zhou, H. Wu, T. J. Udovic and T. Yildirim, *Chem. – Eur. J.*, 2011, **17**, 6043.
15. R.-Q. Zhong, R.-Q. Zou, T. Nakagawa, M. Janicke, T. A. Semelsberger, A. K. Burrell and R. E. Del Sesto, *Inorg. Chem.*, 2012, **51**, 2728.
16. X.-l. Si, L.-x. Sun, F. Xu, C.-l. Jiao, F. Li, S.-s. Liu, J. Zhang, L.-f. Song, C.-h. Jiang and S. Wang, *Int. J. Hydrogen Energy*, 2011, **36**, 6698.
17. G. Srinivas, J. Ford, W. Zhou and T. Yildirim, *Int. J. Hydrogen Energy*, 2012, **37**, 3633.
18. G. Srinivas, W. Travis, J. Ford, H. Wu, Z.-X. Guo and T. Yildirim, *J. Mater. Chem. A*, 2013, **1**, 4167.
19. Z. Li, G. Zhu, G. Lu, S. Qiu and X. Yao, *J. Am. Chem. Soc.*, 2010, **132**, 1490.
20. H. M. Jeong, W. H. Shin, J. H. Park, J. H. Choi and J. K. Kang, *Nanoscale*, 2014, **6**, 6526.
21. Z. Li, W. Liu, H. Yang, T. Sun, K. Liu, Z. Wang and C. Niu, *RSC Adv.*, 2015, **5**, 10746.
22. M. Eddaoudi, J. Kim, N. Rosi, D. Vodak, J. Wachter, M. O'Keeffe and O. M. Yaghi, *Science*, 2002, **295**, 469.
23. H. Furukawa, N. Ko, Y. B. Go, N. Aratani, S. B. Choi, E. Choi, A. O. Yazaydin, R. Q. Snurr, M. O'Keeffe, J. Kim and O. M. Yaghi, *Science*, 2010, **329**, 424.
24. M. Savonnet, D. Bazer-Bachi, N. Bats, J. Perez-Pellitero, E. Jeanneau, V. Lecocq, C. Pinel and D. Farrusseng, *J. Am. Chem. Soc.*, 2010, **132**, 4518.
25. C. J. Doonan, W. Morris, H. Furukawa and O. M. Yaghi, *J. Am. Chem. Soc.*, 2009, **131**, 9492.
26. S. J. Garibay and S. M. Cohen, *Chem. Commun.*, 2010, **46**, 7700.
27. P. A. P. Mendes, F. Ragon, A. E. Rodrigues, P. Horcajada, C. Serre and J. A. C. Silva, *Microporous Mesoporous Mater.*, 2013, **170**, 251.
28. L. Shen, W. Wu, R. Liang, R. Lin and L. Wu, *Nanoscale*, 2013, **5**, 9374.
29. F. Vermoortele, R. Ameloot, A. Vimont, C. Serre and D. De Vos, *Chem. Commun.*, 2011, **47**, 1521.
30. A. Staibitz, A. P. Robertson, M. E. Sloan and I. Manners, *Chem. Rev.*, 2010, **110**, 4023.
31. W. J. Atkins, E. R. Burkhardt and K. Matos, *Org. Process Res. Dev.*, 2006, **10**, 1292.
32. E. J. Corey, R. K. Bakshi and S. Shibata, *J. Am. Chem. Soc.*, 1987, **109**, 5551.
33. S. Horike, M. Dinca, K. Tamaki and J. R. Long, *J. Am. Chem. Soc.*, 2008, **130**, 5854.
34. J. M. Roberts, B. M. Fini, A. A. Sarjeant, O. K. Farha, J. T. Hupp and K. A. Scheidt, *J. Am. Chem. Soc.*, 2012, **134**, 3334.
35. A. V. A. Kumar and S. K. Bhatia, *Phys. Rev. Lett.*, 2006, 96.
36. N. M. Yoon, C. S. Pak, H. C. Brown, S. Krishnam and T. P. Stocky, *J. Org. Chem.*, 1973, **38**, 2786.
37. C. Ollivier and P. Renaud, *Chem. Rev.*, 2001, **101**, 3415.
38. P. Renaud, A. Beauseigneur, A. Brecht-Forster, B. Becattini, V. Darmency, S. Kandhasamy, F. Montermini, C. Ollivier, P. Panchaud, D. Pozzi, E. M. Scanlan, A.-P. Schaffner and V. Weber, *Pure Appl. Chem.*, 2007, **79**, 223.
39. A. D. Sutton, A. K. Burrell, D. A. Dixon, E. B. Garner, J. C. Gordon, T. Nakagawa, K. C. Ott, J. P. Robinson and M. Vasiliu, *Science*, 2011, **331**, 1426.

